UWB RAKE RECEIVER PERFORMANCE ANALYSIS FOR TWO DIFFERENT MODULATION TECHNIQUES

Florin CRĂCIUN[1]

Sistemele de comunicaţii de banda ultralargă (ultra wideband – UWB) se dovedesc a fi sisteme noi şi sigure pentru comunicaţiile fără fir, datorită capacităţii lor de a asigura comunicaţii de putere scăzută, cu rată mare de transmisie pe distanţe scurte, într-un mediu aglomerat în care avem un număr mare de căi multiple de propagare. Vom analiza şi compara performanţele a trei tipuri de receptoare RAKE (RAKE ideal, RAKE selectiv şi RAKE parţial) şi a două tipuri de tehnici de modulaţie TH-PPM şi TH-PAM în acest mediu.

Ultra wideband (UWB) communication systems prove to be new and reliable systems for wireless communications due to their capacity to provide low power, short range high date rate, fade free, relatively shadow-free communications in a dense multipath environment. We shall analyze these performances of three different type of RAKE receivers (Ideal RAKE, Selective RAKE and Partial RAKE) and two different modulation techniques TH-PPM and TH-PAM.

Keywords: spread spectrum, time hopping, ultra-wideband modulation, RAKE receiver

1. Introduction

UWB is defined as any radio technology having a spectrum that occupies a bandwidth greater than 20 percent of the center frequency, or a bandwidth of at least 500 MHz [1]. There are many types of UWB systems which are using the 3.1 – 10.6 GHz unlicensed spectrum: time-hopping spread spectrum impulse radio, direct sequence spread spectrum impulse radio [2].

UWB communication systems are based on impulse radio and uses waveforms that consist of trains of very narrow pulses, nanoseconds wide. These baseband pulses spread the energy of the radio signal over few GHz. For a UWB pulse we considered the second derivate of a Gaussian function $\exp\left(-2\pi\left[\frac{t}{t_n}\right]^2\right)$

[1] PhD student, Electronics, Telecommunications and Information Technology Faculty, University POLITEHNICA of Bucharest, Romania, e-mail: fcraciun@yahoo.com

$$\omega = \left[1 - 4\pi\left[\frac{t}{\tau}\right]^2\right]\exp\left(-2\pi\left[\frac{t}{\tau}\right]^2\right) \quad (1)$$

where τ is a shape factor . In Fig. 1 it is plotted a Gaussian impulse for three values of τ and in Fig. 2 is represented the power spectrum of impulse radio for the same three values of the shape factor τ .

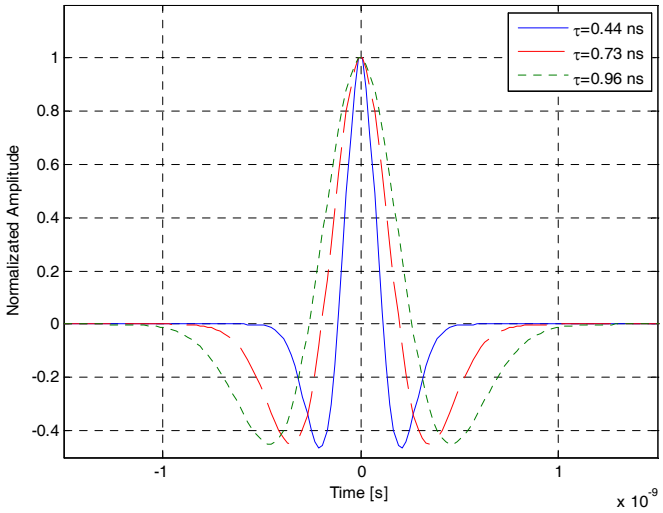

Fig. 1. The waveforms impulse radio based on second derivate of a Gaussian function for three values of the shape factor τ

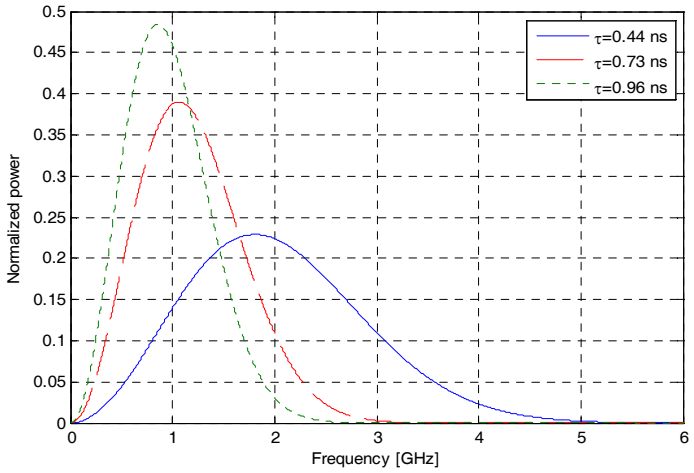

Fig. 2. The power spectrum of impulse radio based on second derivate of a Gaussian function for three values of the shape factor τ

2. Time Hopping Signals

Impulse radio, operating in the highly populated frequency range below a few gigahertzes must content with a variety of interfering signals and also must insure that they do not interfere with narrowband radio systems operating in dedicated bands. These requirements necessitate the use of spread-spectrum techniques. A simple means for spreading the spectrum of these ultra wide bandwidth low-duty-cycle pulse trains is time hopping, with data modulation at the rate of many pulses per data symbol.

A typical time hopping format with pulse position data modulation (PPM) [3] is given by:

$$x^{(\upsilon)}(t) = \sum_{k=0}^{\infty} \omega(t - kT_f - c_k^{(\upsilon)} T_c - \delta^k_{d^{(\upsilon)}_{[k/Ns]}}) \tag{2}$$

where: superscript υ represent a particular user. So the signal emitted by the υ-th user is a large number of monocycle waveforms shifted to different times; the transmitted pulse $\omega_{tx}(t)$ is referred to as a monocycle. The frame time or pulse repetition time T_f typically may be a hundred to a thousand time the monocycle wide. The result is a signal with a very low duty cycle. Time hopping codes $\{c_k^{(\upsilon)}\}$ are periodic pseudorandom codes with period N_p, i.e., $c^{(\upsilon)}_{k+iN_p} = c_k^{(\upsilon)}$ for all integers *i* and *k*.

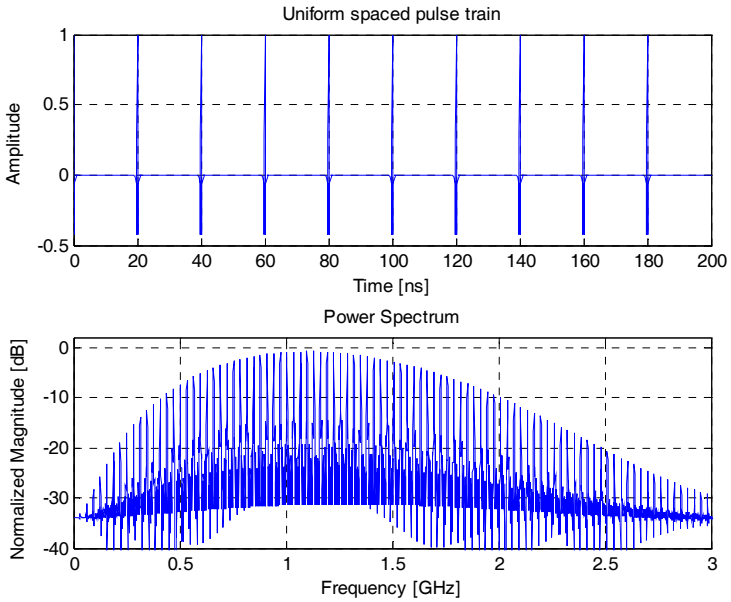

Fig. 3. A uniform spaced monocycle pulse train and its power spectrum.

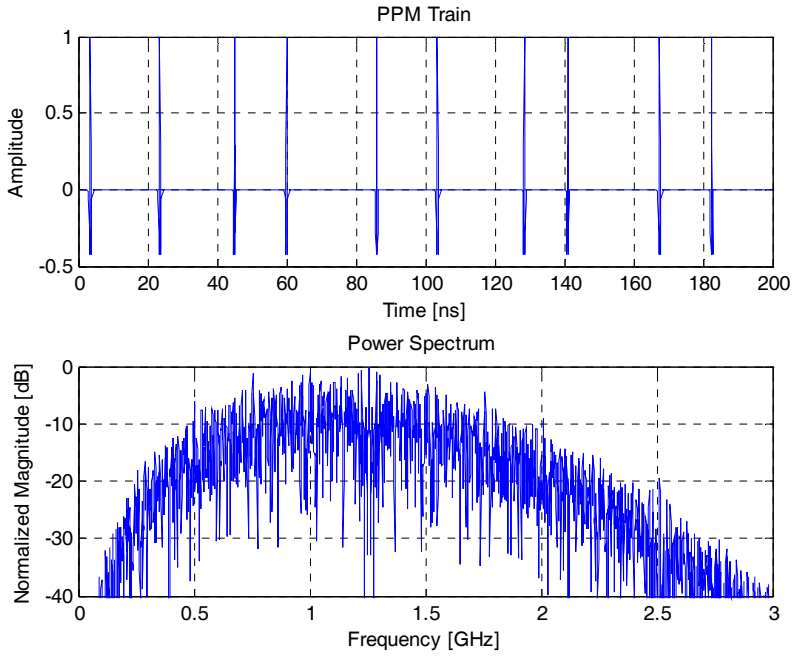

Fig. 4. Randomize pulse train and its power spectrum for PPM signals

One effect of the hopping code is to reduce the power spectral density from the line spectral density ($1/T_f$ apart) of uniformly spaced pulse train, as we can see in Fig. 3, with finer line spacing $1/T_p = 1/N_p T_f$ apart, as we can see in Fig. 4.

Comparison of Fig. 3 and 4 indicates that when the pulse position signals are not randomized the power spectrum is dominated by spectral lines whereas the use of the randomization reduces the lines and the power spectrum is predominately continuous.

The data sequence $\left\{d_i^{(\upsilon)}\right\}$ of user υ is *M*-ary ($1 \le d_m^{(\upsilon)} \le M$) symbol stream that convey information in some form. So the information is carried using the above pulse train by modifying the pulse position (pulse position modulation).It should be noted that the pulse time delay introduced due to modulation is relatively small compared with the time delay resulting from pulse spreading with the spreading code (pulse randomization), so the effects of pulse position modulation on the power spectrum are insignificant.

If we consider an impulse radio with pulse amplitude modulation (PAM) the resulting signal is a PAM-TH-UWB signal which is given by:

$$x^{(\upsilon)}(t) = \sum_{k=0}^{\infty} a_k^{(\upsilon)} \omega(t - kT_f - c_k^{(\upsilon)} T_c) \tag{3}$$

In Fig. 5 we can see a train pulse for PAM-TH-UWB the power spectral density for PAM-TH-UWB after spreading code and modulated data. For the spreading code are valid the same arguments as in the PPM case. The data sequence for user υ is transmitting by modulating the amplitude with the help of the $\left\{a_k^{(\upsilon)}\right\}$ parameter which has the value 1 when a "1" bit is transmitted and value -1 when a "0" bit is transmitted.

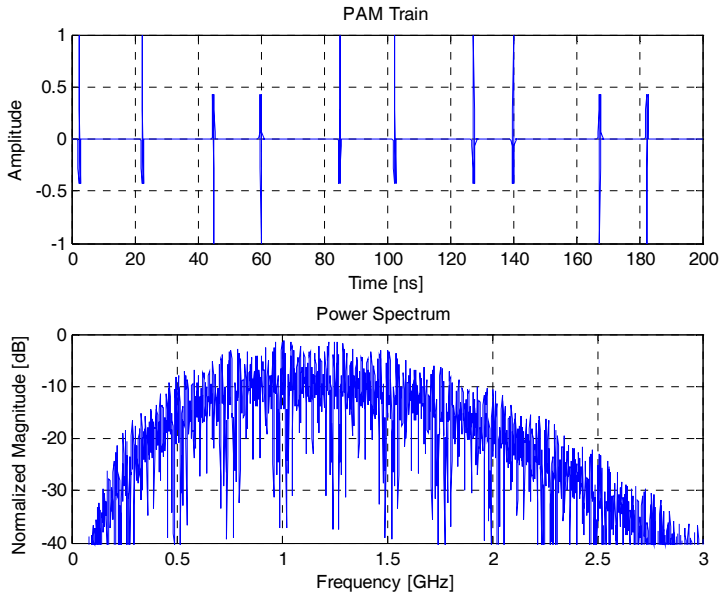

Fig. 5. Randomize pulse train and its power spectrum for PAM signals

3. Channel model

The channel model is based on Saleh-Valenzuela model [5], modified so that multipath gains have a lognormal distribution rather than a Rayleigh distribution. There are four channel models for different propagation environments:

CM1: channel model 1, used for line of sight (LOS) scenario with a distance between the transmitter and the receiver smaller than 4 meters.

CM2: channel model 2, used for a non line of sight (NLOS) scenario with a distance between the transmitter and receiver smaller than 4 meters.

CM3: channel model 3, used for a non line of sight (NLOS) scenario with a distance between the transmitter and receiver between 4 and 10 meters.

CM4: channel model 4, used for an extreme non line of sight (NLOS) scenario with 25 ns RMS delay spread.

We use the following definition for the proposed model:

T_l = the arrival of the first path of the *l*-th cluster

$\tau_{k,l}$ = the delay of the *k*-th cluster path within the *l*-tj cluster relative to the first path arrival time, T_l. By definition, $\tau_{0,l} = 0$.

Λ = cluster arrival rate

λ = ray arrival rate, meaning the arrival rate of path within each cluster.

Table 1

Multipath target characteristic model parameters and model characteristic

	CM1	**CM2**	**CM3**	**CM4**
τ_m [ns[(means excess delay)	5.05	10.38	14.18	
τ_{rms} [ns] (rms delay spread)	5.28	8.03	14.28	25
NP (85%) (number of paths that capture 85% of channel energy)	24	36.1	61.54	
MODEL PARAMETERS				
Λ [1/nsec] (cluster arrival rate)	0.0233	0.4	0.0067	0.0067
λ [1/nsec] (ray arrival rate)	2.5	0.5	2.1	2.1
Γ (cluster delay factor)	7.1	5.5	14	24
γ (ray delay factor)	4.3	6.7	7.9	12
σ_1 [dB] (stand dev. of cluster lognormal fading term in dB)	3.4	3.4	3.4	3.4
σ_2 [dB] (stand dev. of ray lognormal fading term in dB)	3.4	3.4	3.4	3.4
σ_x [dB] (stand dev. of lognormal fading term for total multipath realization in dB)	3	3	3	3
MODEL CHARACTERISTIC				
τ_m	5.0	9.9	15.9	30.1

τ_{rms}	5	8	15	25
NP_{10dB} (number of paths within 10 dB of the strongest paths)	12.5	15.3	24.9	41.2
NP (85%)	20.8	33.9	64.7	123.3
Channel energy mean [dB]	-0.4	-0.4	0.0	0.3
Channel energy std dev. [dB]	2.9	3.1	3.1	2.7

Table 1 contains the channel target characteristic, model parameters and model characteristic for these channels.

Because of the very short distance between the transmitter and the receiver, the terminal mobility in very limited and thus the model assumes the channel to be time-invariant within the transmission of each packet.

Impulse response is modeled by the following equation:

$$h_i(t) = X_i \sum_{l=0}^{L} \sum_{k=0}^{K} \alpha_{k,l}^{i} \delta(\tau - T_l^i - \tau_{k,l}^i) \tag{4}$$

where :

$\alpha^{i}_{k,l}$ - are the multipath gain coefficients, T_l^i is the delay of the *l*-th cluster, $\tau^{i}_{k,l}$ is the delay of the *k*-th multipath component relative to the *l*-th arrival time (T_l^i), X_i represents the log-normal shadowing , and i refers to the *i*-th realization .

Based on this parameters and characteristics we simulate the impulse response on these channel models and obtained the graphics in Fig. 6.

As we can see, in the case of CM1 channel (LOS case), the main component is the first component and there are few other delayed replicas. In the case of CM4 (extreme NLOS case), the main components are the delayed components. We can observe that there are important components even after 100 ns from the first contribution. In this case the receiver should try to collect all the components to perform the correct detection and decoding. Such a receiver is known as RAKE receiver.

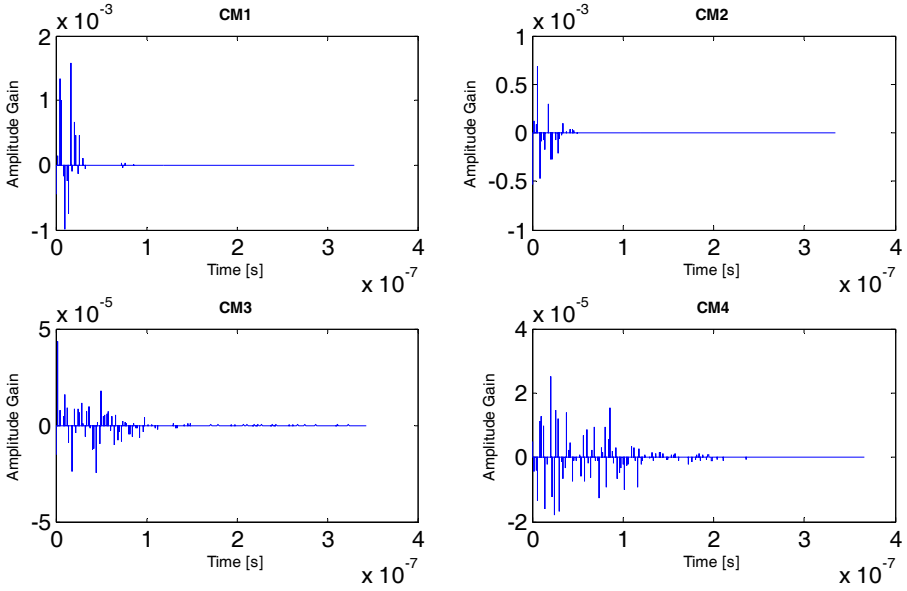

Fig. 6. Impulse response based on CM1-4 channel model in a period

4. RAKE Receiver

The received signal IR transmissions can be modeled as:

$$r(t) = X\sqrt{E_{TX}}\sum_j \sum_{n=1}^{N}\sum_{k=1}^{K(n)} \alpha_{nk} a_j \omega_0 \left(t - jT_s - \varphi_j - \tau_{nk}\right) + n(t) \qquad 5)$$

where:

X is the log-normal distributed amplitude gain of the channel, E_{TX} is the transmitted energy per pulse, N is the number of clusters observed at destination, $K(n)$ is the number of multi-path contributions associated with the n-th cluster, α_{nk} is the channel coefficient of the k-th path within the n-th cluster, a_j is the amplitude of the j-th transmitted pulse (a_j=1 in case of PPM), T_s is the average pulse repetition period, φ_j is the time dithering associated to the j-th pulse , τ_{nk} is the delay of the k-th path associated within the n-th cluster.

The energy contained in the channel coefficients α_{nk} is normalized to unity for each realization of the channel impulse response, that is:

$$\sum_{n=1}^{N}\sum_{k=1}^{K(n)} \left|\alpha_{nk}\right|^2 = 1 \qquad (6)$$

And equation (5) can be rewritten as follows:

$$r(t) = \sqrt{E_{RX}} \sum_j \sum_{n=1}^{N} \sum_{k=1}^{K(n)} \alpha_{nk} a_j \omega_0 \left(t - jT_s - \varphi_j - \tau_{nk}\right) + n(t) \qquad (7)$$

where $E_{RX} = X^2 E_{TX}$ is the total energy for one transmitted pulse. Different from AWGN channel, E_{RX} is spread in time over the different multi-path contributions and can be used by the detector if the receiver is capable of capturing all replicas of the same pulse. Realistically, the receiver can only analyze a finite subset of N_R contributions, and the effective energy E_{eff}, which is used in the decision process, is smaller than E_{RX}, that is:

$$E_{eff} = E_{RX} \sum_{j=1}^{N_R} \left|\alpha_j\right|^2 \le E_{RX} \qquad (8)$$

According to equation (7) different replicas of the same transmitted pulse overlap at the receiver only when the corresponding inter-arrival time is smaller than pulse duration T_M. In this case signals associated with different paths are not independent, that is, the amplitude of the pulse observed at time *t* is affected by the presence of multi-path contributions arriving immediately before or after time *t*. Given the characteristic of the propagation channel, the number of independent path at the receiver depends on T_M: the smaller T_M, the higher number of independent contributions at receiver input.

At the receiver we implement the Maximal Ratio Combining (MRC). In MRC, the different contributions are weight before the combining and the weights are determined to maximize the SNR before the decision process. Performance of the RAKE receiver for propagation over a multi-path channel [4] ,[7] can be evaluated by first assuming a specific model for the channel impulse response, and by then evaluating the probability of error on the symbol Pr_e as a function of the E_{RX}/N_0 ratio for the different diversity methods. This analysis is performed in general under the hypothesis of perfect knowledge of the coefficients of the channel impulse response, or perfect channel estimation.

The adoption of a RAKE considerably increases the complexity of the receiver. This complexity increases with the number of multi-path components analyzed and combined before decision and can be reduced by decreasing the number of components processed by the receiver. According to equation (8), however, reductions of the number of paths, leads to a decrease of energy collected by the receiver. Different strategies for reducing the complexity of the RAKE are presented and analyzed in terms of Pr_e degradation. The first strategy called Selective RAKE (SRAKE), consists of selecting the L_B best components

among the L_{TOT} available at the receiver input. The number of branches of the RAKE is reduced but the receiver still must keep track of all the multi-path components to perform the selection. A second and simpler solution called Partial RAKE (PRAKE) combines the first arriving L_P paths without operating any selection among all available multi-path components.

The simulation was made under the assumption that we have perfect synchronization between transmitter and receiver. For the propagation environment we used CM4 channel model .We simulated the transmission of 1000 bits and we calculated and plotted the probability of error for different cases.

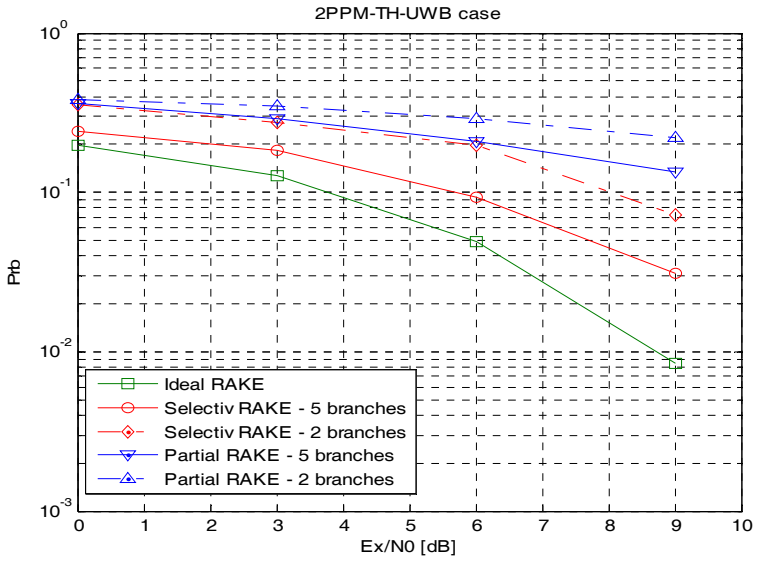

Fig. 7. Probability of error vs signal to noise ratio for 2PPM-TH-UWB case

Fig. 7 compares the performance of the five analyzed RAKE receivers in the case of 2PPM-TH-UWB signals. As expected the best results are obtained with the Ideal RAKE, followed by SRAKE and PRAKE. The loss in performance is about 3 dB for SRAKE with 5 branches and about 6 dB for SRAKE with 2 branches. The simplest solution PRAKE has the poorest performance. We can observe that the 5 braches PRAKE receiver has about the same performances as the SRAKE receiver with 2 branches. In the case of CM4 channel model, the PRAKE solution with 2 branches is unusable because of the poor performance.

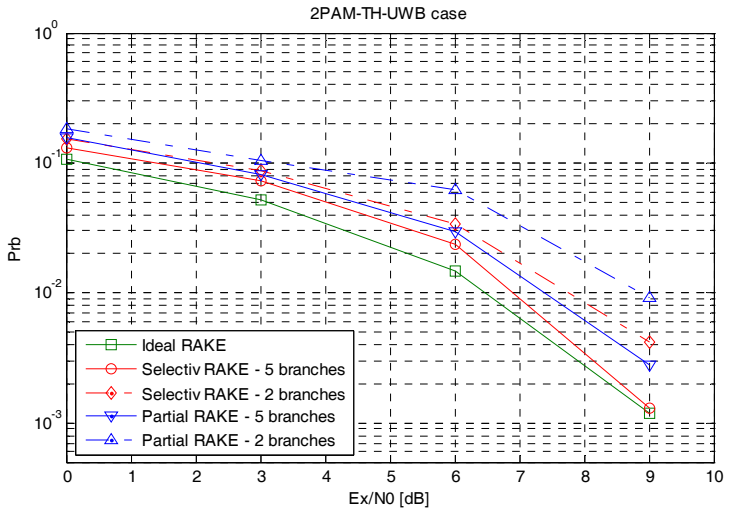

Fig. 8. Probability of error vs signal to noise ratio for 2PAM-TH-UWB case

Fig. 8 compares the performance of the same RAKE receiver in the case of 2PAM-TH-UWB signals. We can observe a similar behavior as in the previous case. As we can see in Fig. 9 the signals based on PAM-TH modulation had better performance than those based on PPM-TH modulation, and the loss in performance for the PPM signals in this case is about 5 dB. This is a general result that derives from the loss of 3 dB in the SNR value suffered by PPM signals

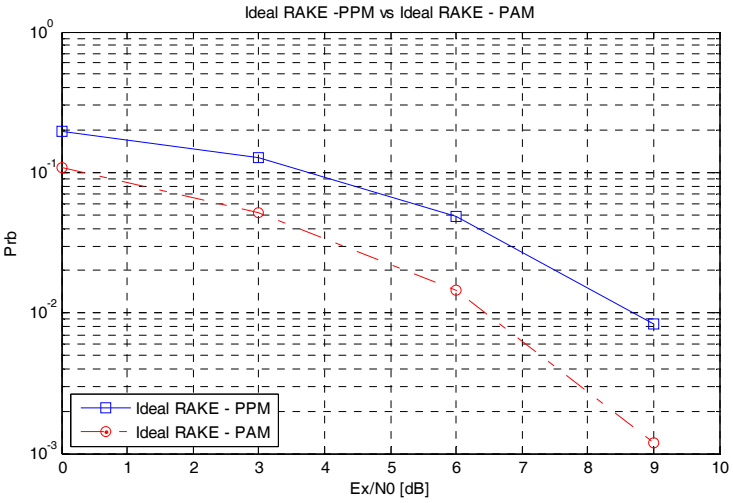

Fig. 9. Performances for an Ideal RAKE receivers for the studied cases.

5. Conclusions

Performances of different types of RAKE receivers were analyzed for two types of modulated signals. The Ideal RAKE receiver has the best performances, but it is not a solution for a practical implementation because we have to take into consideration all the replicas of the transmitted signal. Solutions are SRAKE and PRAKE receivers. Depending on the complexity of the receiver we want to implement and the performances we want to achieve, we can choose one or another RAKE receiver. As expected, SRAKE outperforms PRAKE since it achieves higher SNR at the output of the combiner. The gap in performance, however, decreases when the best paths are located at the beginning of the channel impulse response as it happens in general when considering LOS scenarios. However, in a NLOS channel, like the one we simulated, we can observe that a 2 branches SRAKE receiver has the same performances as a 5 branches PRAKE receiver. In the term of modulation techniques we observed that the 2PAM-TH-UWB signals are more robust than 2PPM-TH-UWB signals.

R E F E R E N C E S

[1]*H. Nikookar and R. Prasad*, "Introducation to Ultra-wideband for wireless communication", Springer ,2009.

[2] *M.Z. Win, R.A. Scholtz* ," Impulse radio: How it works", in IEEE Communication Letter, **vol2**., nr.2, February 1998

[3] *Mohammad Abtahi and Amir R. Forouzan*, "Performance Evaluation of PPM TH-UWB Systems in Indoor Multipath Fading Channels"; International Symposium on Telecommunications; September 2005.

[4] *Arjunan Rajeswaran and V. Srinivasa Somayazulu*, "Rake Performance for a Pulse Based UWB System in a Realistic UWB Indoor Channel"; IEEE Proc. ICC '03, **vol. 4**, p.p. 2879–2883 May 2003.

[5] *A. Saleh and R. Valenzuela*, "A Statistical Model for Indoor Multipath Propagation," IEEE JSAC**, Vol. SAC-5**, No. 2, pp. 128-137, Feb. 1987.

[6] *M.Z. Win, R.A. Scholtz*, "Ultrawide bandwidth time-hopping spread spectrum impulse radio for wireless multiple-access communications", in IEEE Trans. Commun., **vol 48**, no 4, pp. 679-691, April 2000

[7] *M. Z. Win, George Chrisikos, and Nelson R. Sollenberger*, "Performance of Rake reception in dense multipath channels: Implications of spreading bandwidth and selection diversity order," IEEE JSAC, **Vol. 18**, No. 8, pp. 1516-1525, Aug. 2000.

[8] *M. G. Benedetto, T. K. A. F. Molish, L. Oppermann, C. Politano, and D. Porcino*, "UWB Communication Systems A Comprehensive Overview" Hindawi Publishing Corporation, 2006.

[9] *Anderas F. Molisch, Jeffrey R. Foerster, Marcus Pendergrass*, "Channel Models for Ultra-wideband Personal Area Networks", IEEE Wireless Communications, Dec 2003.

[10] *F. Crăciun, O. Fratu, S. Halunga* – „Propagation Channel Simulations for UWB Communications", Telecommunications in Modern Satellite, Cable and Broadcasting Services, 2005. 7th International Conference on ,TELSIKS 2005, **vol. 1,**pag.: 28 – 31,

[11] *F. Crăciun, O. Fratu, S. Halunga* – „On the UWB Perfect Rack receiver performances for different set of spreading codes", Proceedings IEEE ISSCS 2005, **vol. 2**, pag. 657-6